RSC Advances

PAPER

View Article Online
View Journal | View Issue

Cite this: *RSC Adv.*, 2025, **15**, 37965

Nanocomposites based on a multicomponent polyurethane/poly(hydroxypropyl methacrylate) polymer matrix and nanofiller hydroxy-POSS as potential noise and vibration damping materials

Lyudmyla Karabanova, *[a] Nataliia Babkina,[a] Dmytro Klimchuk[b] and Lyubov Honcharova[a]

Received 21st May 2025
Accepted 24th September 2025

DOI: 10.1039/d5ra03574k

rsc.li/rsc-advances

Nanocomposites based on multicomponent polymer matrices, consisting of polyurethane and poly(hydroxypropyl methacrylate) and representing a semi-interpenetrating polymer network, and nanofiller hydroxy-POSS were synthesized, and the thermodynamic parameters of interactions in the system, the dynamic-mechanical properties and the morphology were investigated. The free energy (Gibbs energy) of polyurethane and poly(hydroxypropyl methacrylate) mixing was calculated depending on the hydroxy-POSS content in the nanocomposites. It was shown that polyurethane and poly(hydroxypropyl methacrylate) are thermodynamically incompatible. Introduction of a hydroxy-POSS nanofiller leads to an increase in the thermodynamic incompatibility between polyurethane and poly(hydroxypropyl methacrylate). Dynamic mechanical analysis has shown that for the nanocomposites, there is one maximum of the mechanical loss (tg δ), which is the result of forced phase compatibility and the existence of a large proportion of interphase layers in the systems. This broad maximum of tan δ covers the temperature range from 0 to 100 °C and has a rather high intensity. This means that the created nanocomposites have the potential of being used as effective noise-vibration-damping materials.

Introduction

Polyhedral oligomeric silsesquioxanes (POSS) have attracted considerable attention in the creation of nanocomposites because the organic substituents in the outer layer of POSS molecules make them compatible with polymers, biological systems, and various surfaces.[1–3] Polyhedral oligomeric silsesquioxanes are organosilicon nanoparticles with a size of 1 to 3 nm and a cubic structure that can contain reactive groups allowing for the introduction of POSS into the polymer systems.[4–8] The reactive groups in the outer layer of POSS molecules can be hydroxyl, amine, acrylate, epoxy, and carboxylic acid groups.[9–11] The variety of reactive groups in the outer layer of POSS has made it possible to create nanocomposites and hybrids using POSS for various applications. These can be multifunctional materials from polymer systems to ceramics.

Depending on how many reactive functional groups are there in the POSS, the POSS particle can be embedded in the main polymer chain,[12] form a three-dimensional system,[13] or be suspended from a polymer chain.[12,14] Compared to traditional polymers, materials containing POSS have significant advantages: chemical stability, thermal conductivity, increased hydrophobicity, mechanical strength, hardness, and increased thermal decomposition temperature.[3–8,15]

An essential part of the nanotechnology field is the nanocomposites, which are produced based on polymer matrices. In particular, traditional polyurethanes (PUs), due to the ability to widely vary their composition and properties, are currently one of the most popular classes of polymers, and their demand continues to grow.[16,17] PU materials are widely used in technical and biomedical industries, in particular, in blood contact devices, organ reconstruction,[18] skin coatings and catheters.[19,20] PU is considered an attractive material with a complex structure comprising randomized rigid and flexible nanodomains.[20,21] The addition of functionalized nanofillers can significantly alter its properties. In view of this, polyurethane-based nanocomposites are regarded as promising materials with versatile properties, purposefully tailored through the introduction of nanosized inorganic fillers, such as fullerenes, nanodiamonds, carbon nanotubes and polyhedral oligomeric silsesquioxanes (POSS) into their composition.[20–26]

Studies on polyurethane-matrix nanocomposites containing POSS nanofillers have reported increases in gas transport permeability[27] as well as in conductivity and permeability.[2] The addition of POSS to PU polymers leads to an increase in their

[a]*Institute of Macromolecular Chemistry of National Academy of Sciences of Ukraine, Kyiv, Ukraine. E-mail: lyudmyla_karaban@ukr.net*

[b]*Institute of Botany named M. G. Kholodny of National Academy of Sciences of Ukraine, Kyiv, Ukraine*

thermal stability,[28,29] as well as to an improvement in mechanical properties[30,31] due to the reinforcing effect of nanoparticles. An increase in the oxidation resistance of nanocomposites was also found due to the inclusion of POSS into the systems.[30,32] These beneficial effects were observed mainly when functionalized POSS particles were integrated into polymer chains by a chemical reaction.

In our previous study,[33,34] nanocomposites based on a polyurethane matrix consisting of a trimethylolpropane adduct with toluene diisocyanate (TMP-TDI adduct) and Laprol 5003 as a hydroxyl-containing component were created and investigated. These nanocomposites contained 1,2-propanediolisobutyl-POSS as a functionalized nanofiller. The presence of two reactive hydroxyl groups in the peripheral substituents of this POSS allows them to react with diisocyanates, which promote the incorporation of POSS nanoparticles into the main polymer chain of nanocomposites.[35–37] It was shown that the inclusion of POSS nanoparticles into the PU matrix leads to the formation of a more ordered structure, and also significantly affects the thermal stability of the nanocomposites.[33]

At the same time, multicomponent polymer matrices obtained by the method of interpenetrating polymer networks (IPNs) are quite promising for the creation of the nanocomposites.[38,39] It is known that the majority of synthesized IPNs are phase-separated systems in which microphase separation is the result of the thermodynamic incompatibility of the components.[20,21,24] The presence of microphase separation in the IPNs allows for getting materials in which one of the components plays the role of a matrix or framework, which ensures mechanical strength and physicochemical stability of the system, and the second is a carrier of a certain functionality or specificity of the material. The existence of several levels of chemical and structural heterogeneity in the IPNs can provide additional opportunities for regulating the properties of the nanocomposites. The introduction of nanofillers into such systems can contribute to increasing the compatibility of the polymer components.[40,41] There have been several successful attempts to introduce nanofillers into interpenetrating polymer networks.[42–44]

The aim of this study was to create nanocomposites based on a multicomponent polymer matrix consisting of polyurethane, poly(hydroxypropyl methacrylate), and 1,2-propanediolisobutyl-POSS, which was used as a functionalized nanofiller, and to investigate the effect of POSS content on the thermodynamic of interactions in the systems, dynamic mechanical properties, morphology of the nanocomposites and efficiency of such systems as noise and vibration-damping materials.

Experimental

Materials and methods

The objects of investigations were polyurethane (PU), poly(-hydroxypropyl methacrylate) (PHPMA), semi-IPNs based on them, and nanocomposites containing the functionalized nanofiller 1,2-propanediolisobutyl-POSS with the empirical formula $C_{34}H_{76}O_{15}Si_8$ (Hybrid Plastics Co. Inc.). The polyurethane network for the nanocomposites was formed by a two-stage method. As the isocyanate component, an adduct of trimethylolpropane with toluene diisocyanate (TMP-TDI adduct) was used, which was synthesized at the first stage according to the method.[45] As the hydroxyl-containing component for the formation of the PU network, the bifunctional polyester poly(diethylene glycol) adipate with a molecular weight of 2000 (PDEGA 2000) was selected.

The synthesis of the PU network was carried out by the interaction of the TDI-TMP adduct with PDEGA in the ratio NCO/OH = 2.5/1 up to complete conversion of the isocyanate groups. Nanofiller POSS (1,2-propanediolisobutyl-POSS) was introduced into the compositions during the synthesis of the PU network in a concentration series of 1, 3, 5 and 10 wt%. The compositions were cured at a temperature of 80 °C. As a result, films with a thickness of ~1 mm were obtained.

Semi-IPNs were formed by controlled swelling of POSS-containing polyurethane films in hydroxypropyl methacrylate and subsequent UV irradiation. For radical polymerization of the methacrylate network, the initiator 2,2-dimethoxy-2-phenylacetophenone (IRGACURE 651, λ = 340 nm^{-1}) was used, and the time of irradiation was 30 minutes. The ratios of semi-IPN PU/PHPMA = 85/15 and PU/PHPMA = 70/30 were applied for the synthesis of the nanocomposites.

The molecular structure of the components, which were used, is given in Table 1.

Sorption investigations and thermodynamic parameter calculations

The methylene chloride vapor sorption by samples of native polymers and by nanocomposite's samples was studied using a vacuum installation and a McBain balance.[40] The changes in the partial free energy of methylene chloride by sorption (dissolution) $\Delta\mu_1$ were determined from the experimental data using eqn (1):

Table 1 Structural formulas of the nanocomposite's components

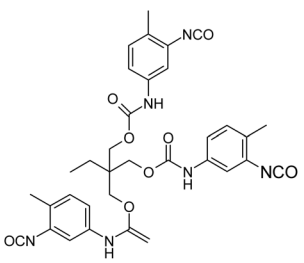

TMP-TDI adduct

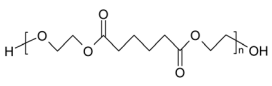

PDEGA 2000

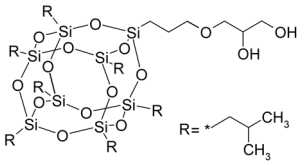

1,2-Propanediolisobutyl-POSS

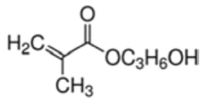

HPMA

$$\Delta\mu_1 = 1/M(\mathrm{RT}\ln P/P_0), \quad (1)$$

where, M is the molecular mass of methylene chloride, and P/P_0 is the relative vapor pressure. The value $\Delta\mu_1$ changes with solution concentration from 0 to $-\infty$.

To calculate the free energy of mixing of the polymer components with the solvent, the changes in the partial free energy of the polymers (native PU, PHPMA, nanocomposites) $\Delta\mu_2$ need to be determined. This requires the calculation of the difference between the polymer chemical potential in the solution of a given concentration and in pure polymer under the same conditions. $\Delta\mu_2$ for the polymer components were calculated using the Gibbs–Duhem equation:

$$w_1(\mathrm{d}\Delta\mu_1/\mathrm{d}w_1) + w_2(\mathrm{d}\Delta\mu_2/\mathrm{d}w_1) = 0, \quad (2)$$

where w_1 and w_2 are the weight fractions of a solvent and of a polymer, respectively. This can be rearranged to give eqn (3):

$$\int \mathrm{d}(\Delta\mu_2) = -\int (w_1/w_2)\mathrm{d}(\Delta\mu_1) \quad (3)$$

Eqn (3) allows the determination of $\Delta\mu_2$ for each polymer from the experimental data by integration over definite limits. The average free energy of mixing of the solvent with the individual PU, PHPMA, and nanocomposites of various compositions for the solutions of different concentrations, was then estimated using eqn (4) and using computational analysis:

$$\Delta g^m = w_1\Delta\mu_1 + w_2\Delta\mu_2 \quad (4)$$

Dynamic mechanical analysis (DMA)

The dynamic mechanical analysis (DMA) measurements were carried out using a Dynamic Mechanical Thermal Analyzer Type DMA Q800 from TA Instruments over the temperature range from −100 to +220 °C and at fixed frequency of 10 Hz with a heating rate of 3 °C min^{-1}. The experiments were performed in the tension mode on rectangular specimens (35 mm × 5 mm × 1 mm). As PHPMA is a hydroscopic polymer, all samples were dried at 80 °C for 48 h under vacuum before measurements. The samples were subsequently subjected to the following thermal cycle during DMA measurements: a first run from +20 °C up to 100 °C, and then second run from −100 °C up to +220 °C. The second run was used for analysis of the results.

Scanning electron microscopy (SEM)

Scanning electron microscopy (SEM) was performed on a JEOL JSM 6060 LA (Tokyo, Japan) at an accelerating voltage of 30 kV and using a detector of secondary electrons. The samples were cut into the strips, before being submerged in liquid nitrogen for 5 min and fractured as quickly as possible. Then, the samples were warmed to room temperature and fixed to an SEM stub. The fracture samples were coated with gold in a vacuum to prevent accumulation of static charge and to increase the resolution. All measurements were done at 20 °C and at magnification of 10 000 and 15 000 times.

Results and discussion

Thermodynamic of interactions in the POSS-containing nanocomposites

The isothermal sorption of methylene chloride vapors by the created systems was studied on purpose to calculate the thermodynamic parameters of interactions between the components of POSS-containing nanocomposites. The aim of the study was to evaluate the influence of the hydroxy-POSS nanofiller on the Gibbs energy, *i.e.* the free energy of polymer components mixing during the formation of semi-IPNs.

The basis for the calculations of the thermodynamic parameters of the polymer component interactions in the nanocomposites was the experimental isotherms of vapors sorption of low molecular weight solvents by the created samples. Fig. 1 shows the isotherms of methylene chloride vapors sorption at 25 °C by samples of the native components of the matrix – PU, PHPMA, by semi-IPNs, consisting of 85% of PU and 15% of PHPMA, and by nanofiller hydroxy-POSS.

It can be seen that the isotherm of methylene chloride vapors sorption by PU (Fig. 1, curve 1) lies higher than the isotherm of methylene chloride vapors sorption by PHPMA (Fig. 1, curve 2). At the same time, vapor sorption by PHPMA almost does not occur until the relative pressure of methylene chloride vapors reaches $P/P_0 = 0.4$. Only after reaching a certain amount of solvent in the polymer volume, the polymer transitions from a glassy state into an amorphous state occurs, after which a rapid increase of vapors sorption by PHPMA begins. This is

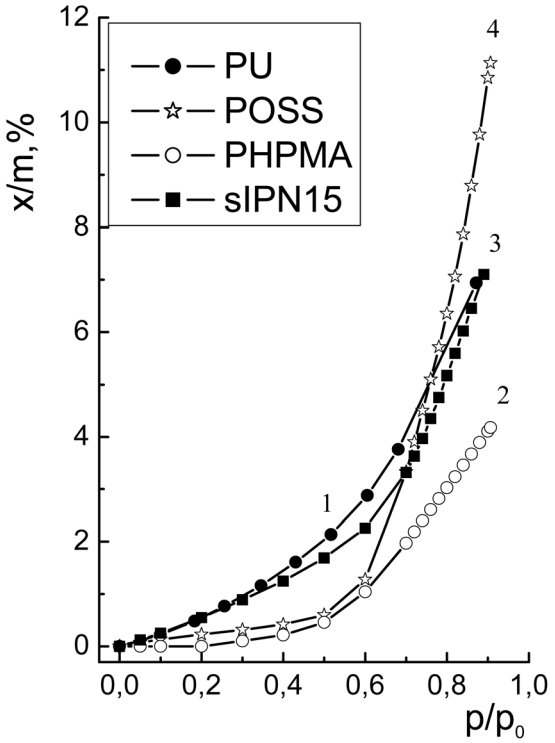

Fig. 1 Isotherms of methylene chloride vapor sorption at 25 °C by samples of the native PU (1), native PHPMA (2), semi-IPNs with composition PU/PHPMA = 85/15 (3), by nanofiller hydroxy-POSS (4).

a typical behavior of polymers in a glassy state.[46] The isotherm of methylene chloride vapor sorption by a sample of semi-IPNs with the composition PU/PHPMA = 85/15 (Fig. 1, curve 3) lies below the isotherm of sorption by PU, but above the isotherm of sorption by PHPMA.

Fig. 2 shows the isotherms of methylene chloride vapor sorption at 25 °C by samples of the semi-IPNs matrix containing 85% of PU and 15% of PHPMA, and by the nanocomposites created on the basis of the semi-IPNs matrix PU/PHPMA = 85/15, and containing hydroxy-POSS as a nanofiller with an amount from 1% to 10% by weight. It can be seen that the sorption capacity of the matrix is the lowest among the studied samples. When the hydroxy-POSS nanofiller is introduced into the system, the sorption capacity of the nanocomposite samples increases compared to the native matrix. We observe that the isotherms of methylene chloride vapor sorption by the nanocomposite samples lie higher than the isotherm of vapor sorption by the semi-IPNs sample. At a qualitative level, this may mean that the samples of the obtained nanocomposites have a less dense structure than the sample of the native matrix. At the same time, the isotherm of vapor sorption by the nanocomposite sample containing 1% POSS lies highest. When the nanofiller content increases to 3–10%, the isotherms of methylene chloride vapor sorption by nanocomposite samples lie lower, *i.e.* they have a denser structure than the nanocomposite with 1% of hydroxy-POSS.

The application of thermodynamic methods to experimental data on the sorption of solvent vapors allows us to estimate a number of system characteristics at a quantitative level. Based on the experimental sorption isotherms, the change in the partial free energy of methylene chloride $\Delta\mu_1$, and the change in the partial free energy of the individual polymer components, semi-IPNs, and nanocomposites upon sorption $\Delta\mu_2$, the average free energy of mixing of individual components and semi-IPNs with the solvent Δg^m for solutions of different concentrations was obtained as described in the Experimental section.

Fig. 3 shows the calculated values of the average free energy of mixing Δg^m of semi-IPNs based on PU and PHPMA, and nanocomposites containing hydroxy-POSS with a solvent. As can be seen, all the studied systems: semi-IPNs – methylene chloride, nanocomposites – methylene chloride, hydroxy-POSS – methylene chloride – are thermodynamically stable $\left(\frac{\partial^2 \Delta g^m}{\partial w_2{}^2} > 0\right)$.[47] At the same time, the affinity of methylene chloride to hydroxy-POSS (Fig. 3, curve 1) is the lowest. Among a series of samples: semi-IPNs and nanocomposites based on semi-IPNs, the affinity of methylene chloride to the polymer matrix is less than to the nanocomposites.

With the introduction of hydroxy-POSS into the matrix, the affinity of methylene chloride to the nanocomposites increases. At the same time, the highest affinity of methylene chloride to the nanocomposites is for the sample with a minimum amount

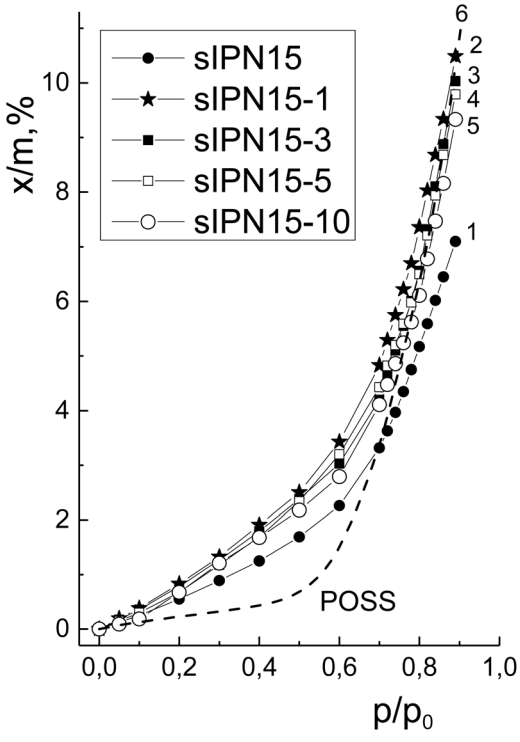

Fig. 2 Isotherms of methylene chloride vapor sorption at 25 °C by samples of the matrix semi-IPNs of the composition PU/PHPMA = 85/15 (1), by the nanocomposites based on the matrix PU/PHPMA = 85/15, containing 1% (2), 3% (3), 5% (4), 10% (5) hydroxy-POSS, by nanofiller hydroxy-POSS (6).

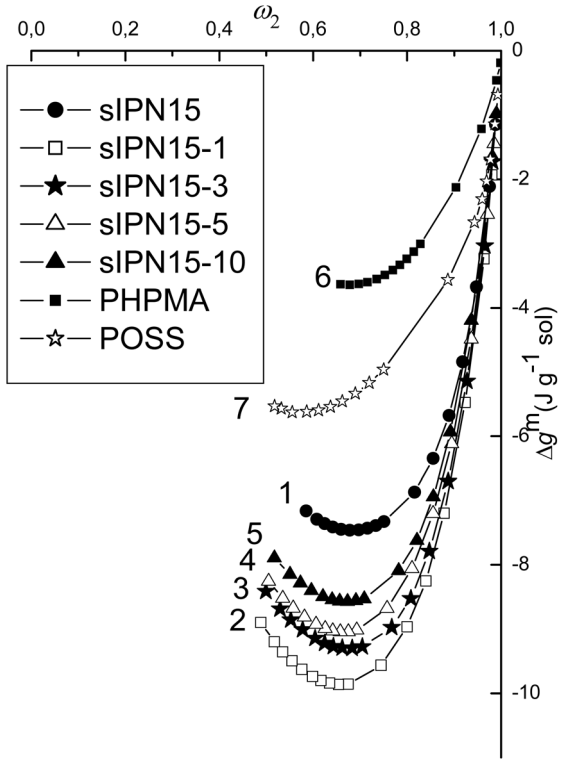

Fig. 3 Concentration dependence of the free energy of polymer–solvent mixing for semi-IPNs of the composition PU/PHPMA = 85/15 (1), nanocomposites based on the matrix PU/PHPMA = 85/15, containing 1% (2), 3% (3), 5% (4), 10% (5) of hydroxy-POSS, for PHPMA (6), for nanofiller hydroxy-POSS (7).

of POSS (1%). With an increase in the amount of hydroxy-POSS in the nanocomposites, the affinity of methylene chloride to the nanocomposites decreases.

Fig. 4 shows the isotherms of methylene chloride vapor sorption at 25 °C by samples of the semi-IPNs matrix containing 70% of PU and 30% of PHPMA, and by the nanocomposites created on the basis of the semi-IPNs matrix PU/PHPMA = 70/30, and containing hydroxy-POSS as a nanofiller with a concentration from 1% to 10% by weight.

It can be seen that the sorption capacity of the matrix semi-IPNs of composition PU/PHPMA = 70/30 (Fig. 4, curve 1) is close to the sorption capacity of matrix semi-IPNs of composition PU/PHPMA = 85/15 (Fig. 2, curve 1). However, the sorption capacity of the nanocomposites based on matrix PU/PHPMA = 70/30 (Fig. 4, curves 2–5) is less than the sorption capacity of the nanocomposites based on matrix PU/PHPMA = 85/15 (Fig. 2, curves 2–5). At a qualitative level, this may mean that the samples of the nanocomposites based on matrix PU/PHPMA = 70/30 have a denser structure than the samples of the nanocomposites based on matrix PU/PHPMA = 85/15.

Fig. 5 shows the calculated values of the average free energy of mixing Δg^m of semi-IPNs based on PU and PHPMA with PU/PHPMA = 70/30, and nanocomposites containing hydroxy-POSS based on matrix PU/PHPMA = 70/30 with a solvent. As could be seen, the affinity of methylene chloride to the matrix PU/PHPMA = 70/30 (Fig. 5, curve 1) is higher than the affinity of methylene chloride to the matrix PU/PHPMA = 85/15 (Fig. 3, curve 1). The affinity of methylene chloride to the nanocomposites (Fig. 5, curves 2–5) is close to the affinity of methylene chloride to the matrix (Fig. 5, curve 1).

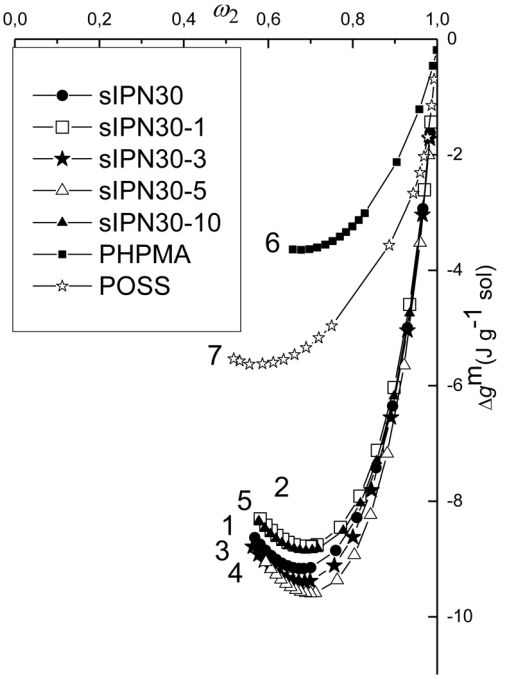

Fig. 5 Concentration dependence of the free energy of polymer–solvent mixing for semi-IPNs of the composition PU/PHPMA = 70/30 (1), nanocomposites based on the matrix PU/PHPMA = 70/30, containing 1% (2), 3% (3), 5% (4), 10% (5) of hydroxy-POSS, for PHPMA (6), for nanofiller hydroxy-POSS (7).

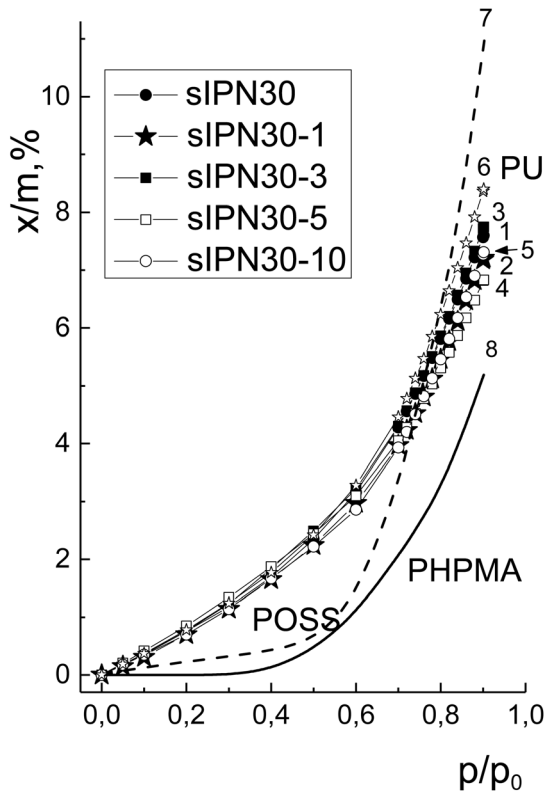

Fig. 4 Isotherms of methylene chloride vapor sorption at 25 °C by samples of the matrix semi-IPNs of the composition PU/PHPMA = 70/30(1), by nanocomposites based on the matrix PU/PHPMA = 70/30 containing 1% (2), 3% (3), 5% (4), 10% (5) of hydroxy-POSS, by sample of PU (6), by sample of hydroxy-POSS (7), by sample of PHPMA (8).

Based on the concentration dependences of Δg^m – the average free energy of mixing of polymer components, semi-IPNS and nanocomposites with methylene chloride, according to the thermodynamic cycles proposed by A. A. Tager and colleagues,[47] the values of the free energy of PU and PHPMA mixing were calculated depending on the hydroxy-POSS content in the nanocomposites. The results of the calculations are given in Table 2.

It can be seen (Table 2) that the free energy of mixing of the samples with methylene chloride at a critical concentration (maximum dilution of the solution) for PU is −13.45 cal g^{-1} of polymer. For PHPMA, this value is −5.23 cal g^{-1} of polymer. That is, the free energy of PU mixing with methylene chloride at a critical concentration is more than twice higher in comparison with the free energy of PHPMA mixing with methylene chloride. For semi-IPNs, which contain 15% of PHPMA, the free energy of mixing with methylene chloride at a critical concentration is −13.11 cal g^{-1} of polymer. When hydroxy-POSS is introduced into the nanocomposites, the free energy of mixing with methylene chloride changes from −18.02 cal g^{-1} of polymer to −15.26 cal g^{-1} of polymer. At the same time, with the hydroxy-POSS content, the free energy of mixing with methylene chloride at a critical concentration decreases.

Table 2 Free energy of polyurethane and poly(hydroxypropyl methacrylate) mixing in the nanocomposites Δg_x depending on the hydroxy-POSS content

Sample composition	Amount of POSS, %	Free energy of mixing with methylene chloride at critical concentration, cal per g polymer	Free energy of PU and PHEMA mixing Δg_x, cal per g polymer
PU	0	Minus 13.45	—
PHPMA	0	Minus 5.23	—
s-IPNs PU/PHPMA 85/15	0	Minus 13.11	Plus 0.91
s-IPNs PU/PHPMA 85/15 + 1% POSS	1	Minus 18.02	Plus 5.98
s-IPNs PU/PHPMA 85/15 + 3% POSS	3	Minus 16.86	Plus 4.66
s-IPNs PU/PHPMA 85/15 + 5% POSS	5	Minus 16.32	Plus 4.12
s-IPNs PU/PHPMA 85/15 + 10% POSS	10	Minus 15.26	Plus 3.06
s-IPNs PU/PHPMA 70/30	0	Minus 15.06	Plus 2.19
s-IPNs PU/PHPMA 70/30 + 1% POSS	1	Minus 14.15	Plus 3.08
s-IPNs PU/PHPMA 70/30 + 3% POSS	3	Minus 15.5	Plus 4.43
s-IPNs PU/PHPMA 70/30 + 5% POSS	5	Minus 15.1	Plus 4.03
s-IPNs PU/PHPMA 70/30 + 10% POSS	10	Minus 14.32	Plus 3.25

For the semi-IPNs, which contain 30% of PHPMA, the free energy of mixing with methylene chloride at a critical concentration is −15.06 cal g^{-1} of polymer. The introduction of hydroxy-POSS leads to a variation of the free energy of mixing with methylene chloride from −14.15 cal g^{-1} of polymer to −15.50 cal g^{-1} of polymer.

Table 2 also shows the calculation results of the free energy of PU and PHPMA mixing during the nanocomposite formation depending on the content of the hydroxy-POSS nanofiller in the systems.

It can be seen (Table 2) that PU and PHPMA are thermodynamically incompatible. The free energy of PU and PHPMA mixing during the formation of the semi-IPNs with 15% PHPMA is positive, but its value is small. When hydroxy-POSS nanofiller is introduced into the semi-IPNs, the free energy of PU and PHPMA mixing remains positive, but increases significantly. This means that the introduction of hydroxy-POSS nanofiller leads to an increase in the thermodynamic incompatibility between PU and PHPMA. At the same time, the highest value of the free energy of mixing was observed for the nanocomposite with the smallest amount of nanofiller −1 wt% of hydroxy-POSS.

When the amount of nanofiller was increased from 3 to 10 wt%, the values of the free energy of mixing slightly decreased in absolute value. That is, with an increase in the amount of nanofiller, the thermodynamic incompatibility between PU and PHPMA decreased. This may be due to the redistribution of the hydroxy-POSS nanofiller between the rigid and flexible nanodomains in the first component of the semi-IPNs – polyurethane.

For semi-IPN with 30% of PHPMA, the free energy of PU and PHPMA mixing during the formation of semi-IPNs is positive. However, the value is higher in comparison with that for the semi-IPN with 15% of PHPMA. This means that with an increase in the amount of PHPMA, the thermodynamic incompatibility between the components of semi-IPNs increases.

As was shown in a previous work,[51] in the study of the thermodynamics of interactions in the nanocomposites based on polyurethane and nanofiller hydroxy-POSS, the free energy of mixing of PU and hydroxy-POSS during the formation of the nanocomposites had positive values at all concentrations of nanofiller. This indicated the thermodynamic incompatibility of the components of nanocomposites based on the PU matrix. This PU matrix is similar to PU, which is a component of the multicomponent matrix studied in this work. It was shown that with an increase in the amount of hydroxy-POSS, the thermodynamic incompatibility decreased a little, and the free energy of PU and hydroxy-POSS mixing during the formation of the nanocomposites remained positive, but decreased in absolute value. It was concluded that this is due to the redistribution of hydroxy-POSS between the rigid and flexible nanodomains of segmented polyurethane, which was the matrix of the nanocomposites. At small concentrations of hydroxy-POSS, it can be incorporated into the polyurethane chain due to the hydroxyls in the side chain of the nanofiller.[52] In this case, it is concentrated in the polyurethane nanodomains, which consist of the isocyanate component of the polymer chain. With increasing hydroxy-POSS concentration, it is partly incorporated into the polymer chain by covalent bonding,[52] but it is also present in the polyurethane matrix as a nanofiller. It is exactly this part

that can be concentrated in the flexible polyurethane nanodomains, which consist of poly(diethylene glycol) adipate polyester with a molecular weight of 2000. This assumption is in good agreement with the results of the nanocomposites study by the method of dynamic mechanical analysis.[51]

Since the nanocomposites investigated in this study were formed on the basis of a multicomponent matrix consisting of PU and PHPMA, and the matrix was formed on the principle of interpenetrating polymer networks of sequential curing, the assumptions made for the nanocomposites based on a polyurethane matrix will also be relevant for nanocomposites based on polyurethane and poly(hydroxypropyl methacrylate) matrix.

Dynamic mechanical properties of the POSS-containing nanocomposites

The influence of the amount of the hydroxy-POSS nanofiller on the segmental motions in the created nanocomposites and on the efficiency of noise and vibration damping of materials was investigated by the method of dynamic mechanical analysis (DMA).

Fig. 6 presents the temperature dependence of the mechanical loss (tan δ) for the native PU, native PHPMA and for the semi-IPNs with the PU/PHPMA = 85/15 ratio, obtained by the DMA method. It can be seen that for the semi-IPNs containing 15% PHPMA, one maximum tg δ is observed, which is located between the maxima for the native polymer components – PU and PHPMA.

According to the results of the thermodynamic parameter calculations of the component interactions in these semi-IPNs (Table 2), the system is thermodynamically incompatible. However, the free energy of PU and PHPMA mixing (Gibbs energy) has a small value (+0.91 cal g^{-1} of polymer). That is, the driving energy required to cause phase separation is insignificant. It is known[48] that interpenetrating polymer networks (or semi-IPNs) begin to form from a thermodynamically compatible system—in our case, a polyurethane network that absorbs the hydroxypropyl methacrylate monomer without the application of an external force. During the formation process of semi-IPNs, as hydroxypropyl methacrylate undergoes photopolymerization within the polyurethane matrix and the second polymer component develops, phase separation begins,[48] but appears to stop at an early stage due to the formation of the network structure. As a result, systems are formed with a large proportion of interphase layers and small phase domains of the semi-IPN components, PU and PHPMA.

It is known[49] that the size of the phase domain of the polymer component, at which its glass transition temperature could be fixed, is at least 15 nm. In cases when microregions with dimensions of 10 nm or less were recorded on scanning electron microscopy images in the polymer blends, all methods of investigations (DMA, DSC, DEA, dilatometry) identified a single glass transition temperature of polymer blends.[50]

From our point of view, one maximum of tg δ for semi-IPNs PU/PHPMA = 85/15 (Fig. 6, curve 3) is the result of forced phase compatibility, or the formation of small-sized phase domains of PU and PHPMA and the formation of a large part of interphase layers, which does not allow for fixing separate peaks of tan δ for PU and PHEMA (that is, glass transitions of PU and PHPMA within the framework of the synthesized semi-IPNs).

Fig. 7 shows the temperature dependence of the mechanical loss (tan δ) for the native PU, native PHPMA, semi-IPNs with the PU/PHPMA = 85/15 ratio (which is the matrix of the nanocomposites), and for the nanocomposites with hydroxy-POSS content from 1% to 10%. It can be seen that the introduction of the hydroxy-POSS nanofiller into the matrix leads to a further shift of the maximum of the tan δ curve in the direction of higher temperatures and decreasing tan δ amplitude.

The shift of the maximum of the tan δ curve in the direction of higher temperatures and decreasing amplitude means that the suppression of the segmental motion in PU is due to the concentration of nanofiller in the flexible segments of PU,[51]

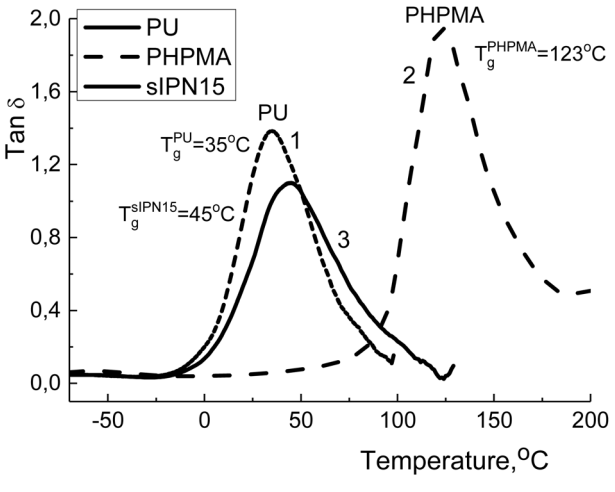

Fig. 6 Temperature dependence of mechanical loss (tan δ) on DMA at a frequency of 10 Hz for the native PU (1), native PHPMA (2) and semi-IPNs with the ratio PU/PHPMA = 85/15 (3).

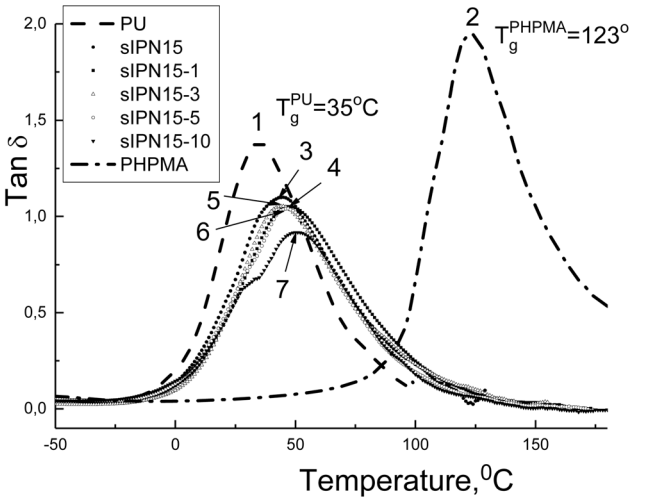

Fig. 7 Temperature dependence of mechanical loss (tan δ) on DMA at a frequency of 10 Hz for PU (1), PHPMA (2), semi-IPNs with the ratio PU/PHPMA = 85/15 (3), and for the nanocomposites containing 1% (4), 3% (5), 5% (6) and 10% (7) of hydroxy-POSS.

resulting in the difficulty of segmental motion. Additionally, Fig. 7 shows that a shoulder appears in the glass transition region of PU on the tan δ curves of the nanocomposites. At small concentrations of hydroxy-POSS, the shoulder is barely noticeable. However, it is clearly visible at 10% of nanofiller. On the tan δ curves of the nanocomposites, the presence of a phase separation is recorded, which is caused by the introduction of hydroxy-POSS into semi-IPNs with the ratio of PU/PHPMA = 85/15.

The thermodynamic parameter calculations of the interactions between the components of the semi-IPNs and the nanocomposites based on it (Table 2) indicate that PU and PHPMA are thermodynamically incompatible. The free energy of PU and PHPMA mixing during the semi-IPNs with 15% PHPMA formation is positive, but its value is small. When the hydroxyl-POSS nanofiller is introduced into the semi-IPNs, the free energy of PU and PHPMA mixing remains positive, but it increases significantly. This means that the introduction of hydroxy-POSS nanofiller leads to an increase in the thermodynamic incompatibility between PU and PHPMA.[51]

This may be due to the redistribution of hydroxy-POSS between the rigid and flexible nanodomains of segmented PU, which is one of the components of the nanocomposite's matrix. At a small concentration of hydroxy-POSS, it can be incorporated into the PU chain due to hydroxyls in the side chain of the nanofiller. At a small amount of hydroxy-POSS, it is concentrated in the rigid nanodomains of PU, which consist of the isocyanate component of the polymer chain.[52]

When the amount of hydroxy-POSS increases, it is partially incorporated into the polymer chain due to covalent bonding. However, it is also present in the PU matrix as a nanofiller. This part of hydroxy-POSS can be concentrated in the flexible nanodomains of PU, which consist of polyester poly(diethylene glycol) adipate with a mol. mass 2000. When the amount of hydroxy-POSS increases to 5–10 wt% in the nanocomposites, a shoulder appears on the tan δ curves of the nanocomposites in the glass transition region of PU (Fig. 7). Obviously, due to the concentration of hydroxy-POSS in the flexible nanodomains of PU, the size of the nanodomains of PU increases and PU begins to demonstrate its glass transition temperature within the framework of the nanocomposites.

Fig. 8 shows the temperature dependences of the mechanical loss (tan δ) for the native PU, native PHPMA, semi-IPNs with a PU/PHPMA ratio of 70/30 (which is the matrix of the nanocomposites), and for the nanocomposites with a hydroxy-POSS content from 1% to 10%.

It can be seen that for the semi-IPNs with a ratio of PU/PHPMA = 70/30, there is one broad maximum of tan δ, which is significantly shifted along the temperature scale towards higher temperatures compared to semi-IPNs with a ratio of PU/PHPMA = 85/15 (from 45 °C to 70 °C). At the same time, for semi-IPNs with a ratio of PU/PHPMA = 70/30, a shoulder is observed in the temperature range of the PU glass transition (Fig. 8, curve 1). That is, with an increase in the content of PHPMA in semi-IPNs up to 30%, the signs of the phase separation are observed in this system, *i.e.* signs of phase separation in the nanocomposite's matrix.

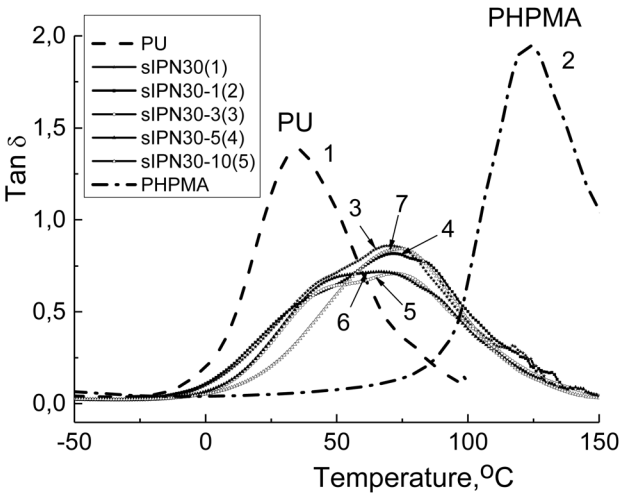

Fig. 8 Temperature dependence of mechanical loss (tan δ) on DMA at a frequency of 10 Hz for PU (1), PHPMA (2), semi-IPNs with a PU/PHPMA ratio of 70/30 (3), and for the nanocomposites containing 1% (4), 3% (5), 5% (6), 10% (7) of hydroxy-POSS.

When the hydroxy-POSS nanofiller is introduced into the matrix at a concentration of 1–3% (Fig. 9b and c), the phase separation in the nanocomposites becomes greater. When 1% of hydroxy-POSS is introduced into the matrix, the shoulder in the glass transition region of PU becomes more clear (Fig. 9b). The introduction of 3% of the nanofiller into the matrix results in two maxima that are observed on the tan δ curve (Fig. 9c). However, when the concentration of hydroxy-POSS increases to 5%, a smoothening of the tan δ curve is observed (Fig. 9d).

As noted above, at a small amount of hydroxy-POSS in the nanocomposites, it can be incorporated into the PU chain due to the hydroxyls in the side chain of the nanofiller. In this case, it is concentrated in the PU nanodomains, which consist of the isocyanate component of the polymer chain.[52] With an increase in the amount of hydroxy-POSS, it is partially incorporated into the polymer chain due to the covalent bonding, but it is also present in the PU matrix as a nanofiller.[51] During the formation of semi-IPNs, hydroxy-POSS, which is not incorporated into the PU chain but is present in the system as a nanofiller, can pass into the interfacial layers of the semi-IPNs. In this case, the phase separation in the system decreases, and a significant part of the interfacial layers is formed. As a result, we observe one broad maximum of tan δ (Fig. 9d), which covers the temperature range from 0 to 100 °C, and has enough high intensity. When 10% of hydroxy-POSS is incorporated into the semi-IPNs matrix with the ratio PU/PHPMA = 70/30, one maximum of tan δ is observed (Fig. 9e). The maximum is narrow and it is shifted towards higher temperatures. In our opinion, this is due to the essential suppression of the segmental motion in the PU. At 10% of nanofiller, it is partially incorporated into the PU chain due to the hydroxyls in the hydroxy-POSS side chain, namely into the rigid nanodomains of PU. A significant part of the nanofiller, which is not incorporated into the rigid nanodomains of PU due to covalent bonding, is concentrated in the flexible nanodomains of PU as a nanofiller. In this case, the

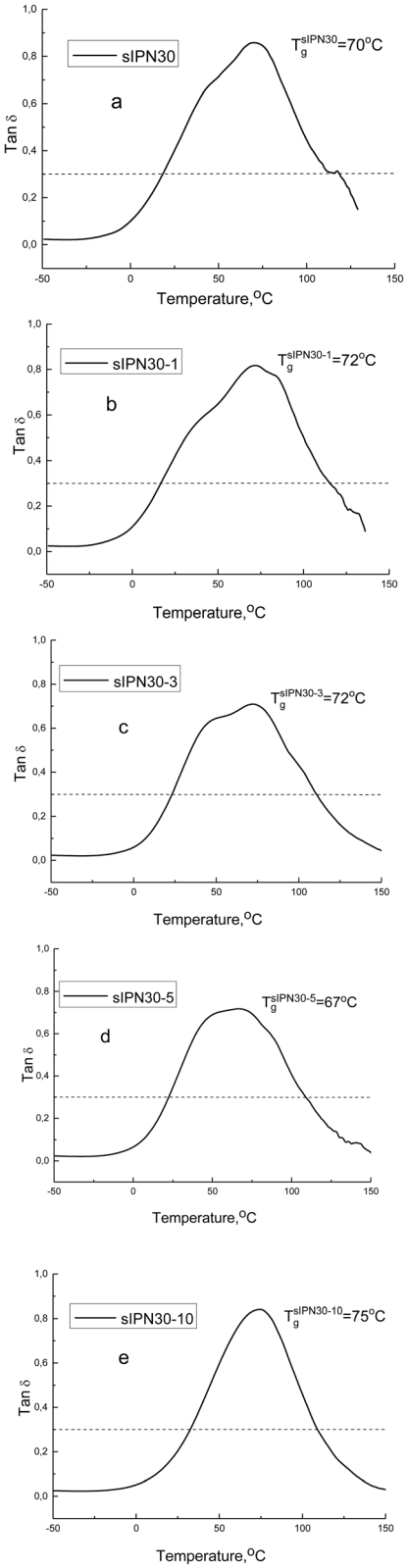

Fig. 9 Temperature dependence of mechanical loss (tan δ) on DMA at a frequency of 10 Hz for the semi-IPNs samples with a PU/PHPMA ratio = 70/30 (a) and for the nanocomposites containing 1% hydroxy-POSS (b), 3% hydroxy-POSS (c), 5% hydroxy-POSS (d), 10% hydroxy-POSS (e).

nanofiller significantly suppresses the segmental motions of the flexible nanodomains in PU. As a result, we observe the tan δ curve (Fig. 9e) for the nanocomposite, in which the segmental motion of the second component of semi-IPNs – PHPMA dominates.

Fig. 10 shows the temperature dependences of the mechanical loss (tan δ) for the nanocomposite based on semi-IPNs with a PU/PHPMA ratio of 70/30, containing 5% of the 1,2-propanediolisobutyl-POSS nanofiller, which were investigated at different frequencies. It can be seen that for this nanocomposite, one broad maximum of tan δ is observed, which shifts along the temperature scale towards higher temperatures as the frequency increases, while the intensity of the maximum of tan δ increases too. Thus, when the frequency changes from 1 Hz to 30 Hz, the tan δ maximum (Tg) shifts from 41 °C to 62 °C, while the intensity of the tan δ maximum increases from 0.7 to 0.85. That is, as the investigation frequency increases, the temperature range of the effective noise and vibration damping expands and shifts toward higher temperatures.

Fig. 11 shows the temperature dependence of the storage modulus for PU (curve 1), PHPMA (curve 2), for semi-IPNs with 15% PHPMA (curve 3) and for the nanocomposites with different amounts of hydroxy-POSS (curves 4–7). Fig. 12 shows the temperature dependence of the storage modulus for the system based on semi-IPNs with 30% PHPMA. We observe that PU is characterized by the minimal storage modulus and PHPMA is characterized by the maximal storage modulus throughout the temperature range. For the semi-IPNs and the nanocomposites, the storage modulus increases in comparison with that for polyurethane. There is a non-monotonic change of the nanocomposite's moduli with the amount of hydroxy-POSS.

Fig. 13 shows the dependence of the relation of the nanocomposites' modulus to the matrix' modulus (Mn/Mo) on the content of the nanofiller. We can observe that the storage moduli of the nanocomposites exceed the storage modulus of the matrix at 1% of hydroxy-POSS. Increasing the hydroxy-POSS

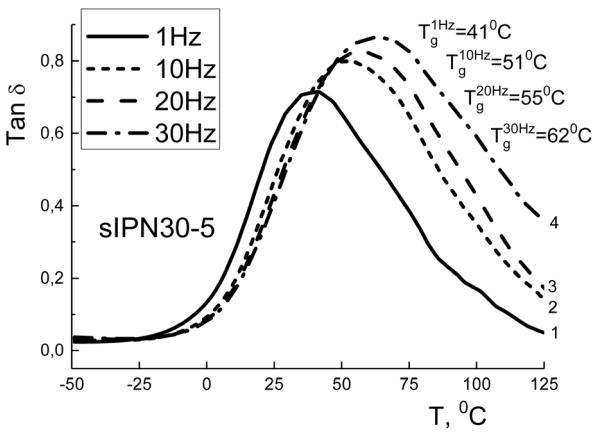

Fig. 10 Temperature dependence of mechanical loss (tan δ) on DMA at different frequencies for the nanocomposite based on the semi-IPNs matrix with a PU/PHPMA ratio = 70/30, containing 5% hydroxy-POSS: 1 Hz (1), 10 Hz (2), 20 Hz (3), 30 Hz (4).

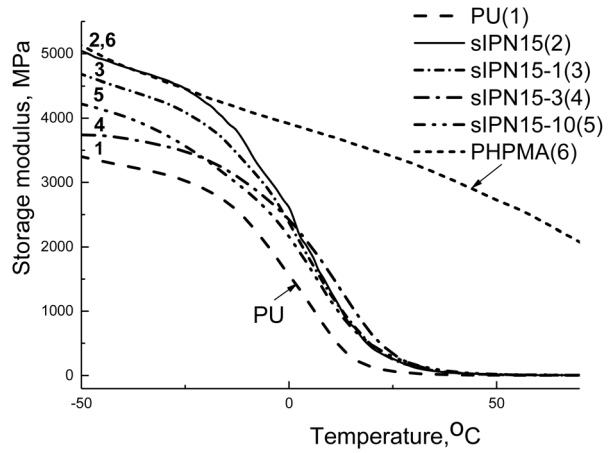

Fig. 11 Temperature dependence of the storage modulus on DMA at a frequency of 10 Hz for PU (1), semi-IPNs with a PU/PHPMA ratio of 85/15 (2) and for the nanocomposites containing 1% (3), 3% (4), 10% (5) of hydroxy-POSS, and of PHPMA (6).

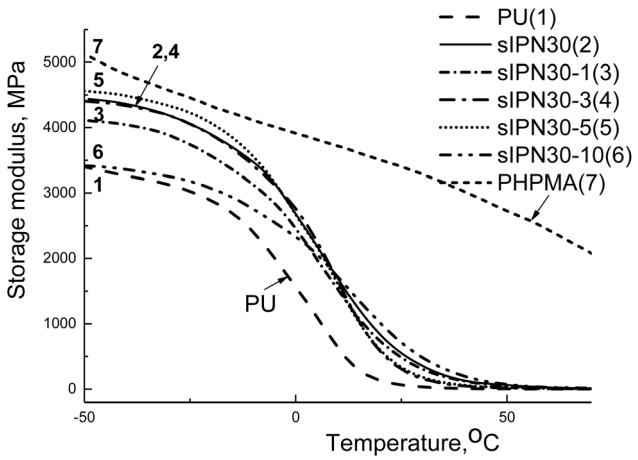

Fig. 12 Temperature dependence of the storage modulus on DMA at a frequency of 10 Hz for PU (1), semi-IPNs with a PU/PHPMA ratio of 70/30 (2) and for the nanocomposites containing 1% (3), 3% (4), 5% (5), 10% (6), and of PHPMA (7).

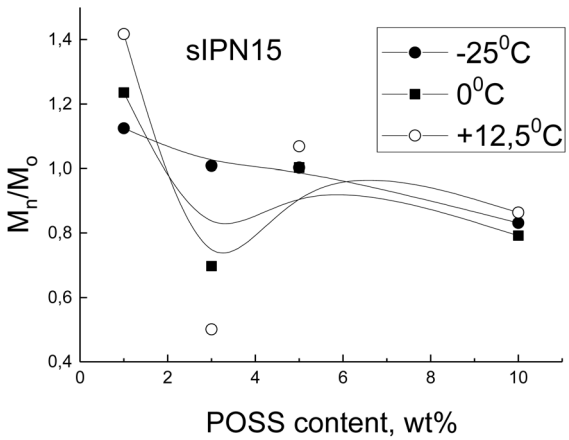

Fig. 13 The relation of the nanocomposite's modulus to the matrix's modulus Mn/Mo *versus* the hydroxy-POSS content at different temperatures – 25 °C (1), 0 °C (2), +12.5 °C (3).

amount in the nanocomposites leads to a decrease of the storage moduli of the nanocomposites, especially at 3% of nanofiller. This could be explained by the thermodynamic peculiarities of the interactions in this system. It was shown (Table 2) that the introduction of the POSS nanofiller leads to an increase in the thermodynamic incompatibility between PU and PHPMA. As a result, we observe a decrease in the modulus of the elasticity of the nanocomposites.

As can be seen from Fig. 7–10, the created materials are effective as noise and vibration damping materials. Effective noise and vibration damping materials are those whose mechanical loss (tg δ) is higher than 0.3.[53–55] In accordance with this criterion, the created materials are effective for damping noise and vibration in a wide range of temperatures (Table 3).

From Table 3, it can be seen that nanocomposites based on a matrix containing 15% PHPMA are effective for noise and vibration damping in the temperature range from 11–14 °C to 89–95 °C. When the content of PHPMA in the matrix of the nanocomposites increases to 30%, the temperature range of the noise and vibration damping shifts to higher temperatures. Such nanocomposites will be effective in the temperature range from 17–33 °C to 110–119 °C. At the same time, with an increase in the amount of hydroxy-POSS nanofiller, the efficiency of the noise and vibration damping shifts toward a higher temperature of about 15 °C.

Thus, POSS-containing nanocomposites based on a multicomponent polymer matrix, consisting of PU and PHPMA and representing a semi-interpenetrating polymer network (semi-IPNs), were synthesized, and the dynamic-mechanical properties of the obtained nanocomposites were investigated. It is shown that for the nanocomposites, one maximum of mechanical loss (tan δ) is observed, which is located between the maxima for the native polymer components. One maximum of tg δ is the result of forced phase compatibility, or the formation of small-sized phase domains of PU and PHPMA and the existence of a large proportion of interphase layers in the systems. This does not allow for fixing the individual glass

Table 3 Maxima of the mechanical loss (tg δ) and the temperature range of effective noise and vibration damping of the created materials

Sample	Max tg δ	Temperature of max tg δ	Effective damping temperature range (tg δ > 0, 3)
PU	1.384	35	6–80
PHPMA	1.945	123	91–175
sIPN15	1.099	45	11–92
sIPN15-1	1.056	44	14–95
sIPN15-3	1.053	45	14–93
sIPN15-5	1.04	47	12–89
sIPN15-10	0.9164	51	13–89
sIPN30	0.8583	70	18–119
sIPN30-1	0.8175	72	17–115
sIPN30-3	0.7194	72	23–111
sIPN30-5	0.7176	70	22–109
sIPN30-10	0.8418	75	33–110

transition temperatures of these components within the synthesized semi-IPNs. The introduction of the hydroxy-POSS nanofiller into the matrix leads to a shift of the tan δ curve towards higher temperatures and to a decrease in its amplitude. This means that there is a suppression of the segmental motion in PU due to the concentration of part of the nanofiller in the flexible segments of PU, resulting in the difficulty of the segmental motion. For nanocomposites based on a matrix with a ratio of PU/PHPMA = 70/30, containing 3% and 5% of hydroxy-POSS, one broad maximum tan δ was found, which covers the temperature range from 0 to 100 °C, and has a rather high intensity of 0.7. This means that the created nanocomposites of the indicated concentrations have the potential of being used as effective noise-vibration-damping materials.

Morphology of the POSS-containing nanocomposites based on polyurethane and poly(hydroxypropyl methacrylate)

Fig. 14 shows the microphotographs of the surface of fresh fractures of samples of the native PU (Fig. 14a), native semi-IPN with 15% of PHPMA (Fig. 14b) and nanocomposites based on semi-IPNs with 15% of PHPMA, containing different amounts of POSS (Fig. 14c–f) at a magnification of 10 000 times.

From the microphotographs, it can be seen that the structures of PU and semi-IPN with 15% of PHPMA are significantly different. The fracture of the PU sample is similar to the fracture of a plastic material, and the structure is sufficiently homogeneous. The morphology of the s-IPNs with 15% of PHPMA (Fig. 14b) presents a non-homogeneous structure with phase inclusions that are about 10 μm. Introduction of POSS nanoparticles into the s-IPN matrix leads to increasing inhomogeneity in the sample structure, especially at 5% and 10% of POSS.

Fig. 15 shows the microphotographs of the surface of fresh fractures of samples of the native PU (Fig. 15a), native semi-IPNs with 30% of PHPMA (Fig. 15b) and nanocomposites based on semi-IPNs with 30% of PHPMA, containing different amounts of POSS (Fig. 15c–f).

From the microphotographs, it can be seen that there are significant differences between the structure of the nanocomposites based on the matrix semi-IPNs with 30% of PHPMA

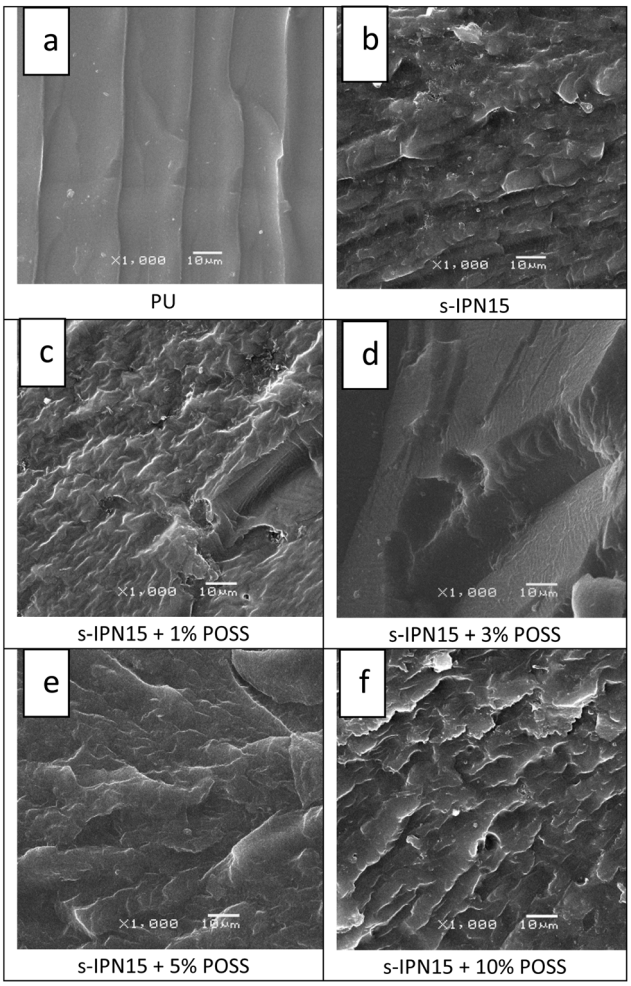

Fig. 14 Microphotographs of polyurethane (a), native semi-IPN with 15% of PHPMA (b) and nanocomposites based on semi-IPN with 15% of PHPMA, containing 1% (c), 3% (d), 5% (e) and 10% (f) of POSS at a magnification of 10 000 times.

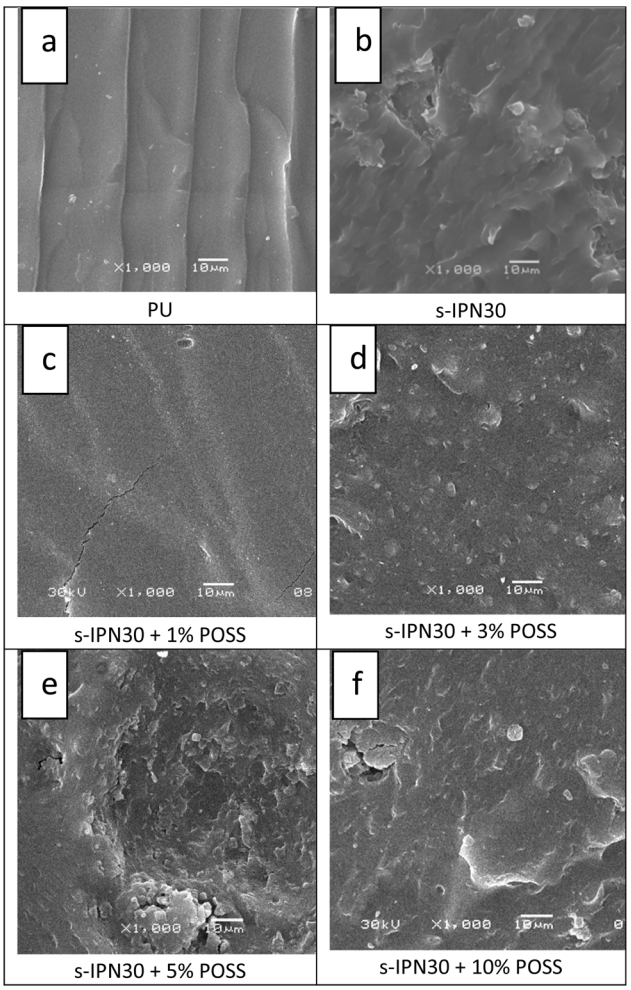

Fig. 15 Microphotographs of PU (a), native semi-IPNs with 30% of PHPMA (b) and nanocomposites based on semi-IPNs with 30% of PHPMA, containing 1% (c), 3% (d), 5% (e) and 10% (f) of POSS at a magnification of 10 000 times.

and that with 15% of PHPMA. For nanocomposites based on matrix semi-IPNs with 30% of PHPMA we could observe phase inclusions of smaller size – 2–5 μm.

The results from the morphology investigations are in agreement with the thermodynamic parameters of interactions in the nanocomposites (Table 2) and with the dynamic-mechanical properties of the nanocomposites (Table 3). In Fig. 15, microphotographs d, e and f show small-sized phase inclusions of PU and PHPMA with significant interphase layers in the systems.

Conclusions

POSS-containing nanocomposites based on a multicomponent polymer matrix consisting of PU and PHPMA and representing a semi-interpenetrating polymer network (semi-IPNs) were synthesized. The thermodynamic parameters of interactions in the system, the dynamic-mechanical properties and the morphology of the obtained nanocomposites were investigated. The free energy (Gibbs energy) of PU and PHPMA mixing was calculated based on experimental data on the sorption of methylene chloride vapors by samples of semi-IPNs and of nanocomposites. It was shown that PU and PHPMA are thermodynamically incompatible. The free energy of PU and PHPMA mixing during the formation of semi-IPNs is positive. Introduction of a hydroxy-POSS nanofiller leads to an increase in the thermodynamic incompatibility between PU and PHPMA. The results of the morphology investigations are in agreement with the thermodynamic parameters of interactions in the nanocomposites. Dynamic mechanical analysis has shown that for the nanocomposites, there is one maximum of the mechanical loss (tan δ), which is located between the maxima for the native polymer components. One maximum of tg δ is the result of forced phase compatibility, or the formation of small-sized phase domains of PU and PHPMA and the existence of a large proportion of interphase layers in the systems, which does not allow for fixing the individual glass transition temperatures of these components within the synthesized semi-IPNs. The introduction of the hydroxy-POSS nanofiller into the matrix leads to a shift of the tan δ curve towards higher temperatures and to a decrease in its amplitude. This means that there is a suppression of segmental motion in PU due to the concentration of part of the nanofiller in the flexible segments of PU, resulting in the difficulty of segmental motion. For nanocomposites based on a matrix with a ratio of PU/PHPMA = 70/30, containing 3% and 5% of hydroxy-POSS, one broad maximum tan δ was found, which covers the temperature range from 0 to 100 °C, and has a rather high intensity of 0.7. A broad maximum of tan δ with high intensity for the nanocomposites means that the created nanocomposites of the indicated concentrations have the potential of being used as effective noise and vibration damping materials.

Author contributions

Lyudmyla Karabanova: conceptualization, supervision, methodology, investigation, data curation, writing – original draft preparation, reviewing and editing. Nataliia Babrina: investigation, writing, reviewing and editing. Dmytro Klymchuk: methodology, investigation, data curation, writing, reviewing and editing. Lyubov Honcharova: investigation, writing, reviewing and editing.

Conflicts of interest

There are no conflicts to declare.

Data availability

The data that support the findings of this study are available from the corresponding author, L. V. Karabanova, upon reasonable request.

Acknowledgements

This study was funded by the National Academy of Sciences of Ukraine, Grant “Scientific principles of functional polymer systems creation for modern technologies”. The received support is gratefully acknowledged.

Notes and references

1 E. Çakmakçi, POSS–Thermosetting Polymer Nanocomposites, in *Polyhedral Oligomeric Silsesquioxane (POSS) Polymer Nanocomposites from Synthesis to Applications*, ed. Thomas, S. and Somasekharan, L., Elsevier, 2021, pp. 127–175, DOI: 10.1016/B978-0-12-821347-6.00004-4.
2 A. A. Fomenko, Yu. P. Gomza, V. V. Klepko, M. A Gumenna, N. S. Klimenko and V. V. Shevchenko, *Polym. J.*, 2009, **31**, 137–143.
3 H. Zhou, M. Chua and J. Xu, Functionalized POSS-based Hybrid Composites, in *Polymer Composites with Functionalized Nanoparticles. Synthesis, Properties, and Applications*, ed. Pielichowski, K. and Majka, T. M., Elsevier, 2019, pp. 179–210, DOI: 10.1016/B978-0-12-814064-2.00006-8.
4 H. Yahyaei and M. Mohseni, Composites and Nanocomposites of PU Polymers Filled With POSS Fillers, in *Polyurethane Polymers*, Elsevier, 2017, pp. 221–252, DOI: 10.1016/B978-0-12-804065-2.00007-3.
5 S. W. Kuo and F. C. Chang, *Prog. Polym. Sci.*, 2011, **36**(12), 1649–1696.
6 Y. P. Gomza, A. A. Fomenko, S. D. Nesin, M. A. Gumenna, N. S. Klymenko, V. V. Shevchenko, and V. V. Klepko, Structure Formation Features of Organic–Inorganic Nanocomposites Based on Silsesquioxanecontaining Polyetherimideurethane, in *Nanosystems, Nanomaterials, Nanotechnologies*, 2008, vol. 6, pp. 965–976, http://dspace.nbuv.gov.ua/handle/123456789/76184.
7 A. Kausar, *Polym.-Plast. Technol. Eng.*, 2017, **56**, 1401–1420.
8 W. P. He, B. Yu Song, Z. Fang and H. Wang, *Prog. Nat. Sci.*, 2020, **114**, 100687.

9 E. Hebda, J. Ozimek, K. N. Raftopoulos, S. Michałowski, J. Pielichowski, M. Jancia and K. Pielichowski, *Polym. Adv. Technol.*, 2015, **26**, 932–940.
10 B. X. Fu, B. S. Hsiao, H. White, M. Rafailovich, P. T. Mather, H. G. Jeon, S. Phillips, J. Lichtenhan and J. Schwab, *Polym. Int.*, 2000, **49**, 437–440.
11 M. Oaten and N. R. Choudhury, *Macromolecules*, 2005, **38**, 6392–6401.
12 W. Zhang, G. Camino and R. Yang, *Prog. Polym. Sci.*, 2017, **67**, 77–125.
13 F. Kazemi, G. Mir Mohamad Sadeghi and H. R. Kazemi, *Eur. Polym. J.*, 2019, **114**, 446–451.
14 M. Joshi, B. Adak and B. S. Butola, *Prog. Nat. Sci.*, 2018, **97**, 230–282.
15 H. Birtane, K. Esmer, S. Madakbas and M. V. Kahraman, *J. Macromol. Sci., Part A*, 2019, **3**, 245–252.
16 D. K Chattopadhyay and D. C. Webster, *Prog. Polym. Sci.*, 2009, **34**, 1068–1133.
17 S. A. Madbouly and J. U. Otaigbe, *Prog. Polym. Sci.*, 2009, **34**, 1283–1332.
18 M. Marzec, J. Kucińska-Lipka, I. Kalaszczyńska and H. Janik, *Mater. Sci. Eng., C*, 2017, **80**, 736–747.
19 A. W. Lloyd, R. G. Faragher and S. P. Denyer, *Biomaterials*, 2001, **22**, 769–785.
20 L. V. Karabanova, A. W. Lloyd, S. V. Mikhalovsky, M. Helias, G. J. Philips, S. F. Rose, L. Mikhalovska, G. Boiteux, L. M. Sergeeva, E. D. Lutsyk and A. Svyatyna, *J. Mater. Sci. Mater. Med.*, 2006, **17**, 1283–1296.
21 V. A. Bershtein, V. M. Gun`ko, L. V. Karabanova, T. E. Sukhanova, P. N. Yakushev, L. M. Egorova, A. A. Turova, V. I. Zarko, E. M. Pakhlov, M. E. Vylegzhanina and S. V. Mikhalovsky, *RSC Adv.*, 2013, **3**, 14560–14570.
22 I. Blanko, Decomposition and ageing of hybrid materials with POSS, in *Polymer/POSS Nanocomposites and Hybrid Materials. Preparation, Properties, Applications*, ed. Kalia, S. and Pielichowski, K., Springer, 2018, pp. 415–462.
23 E. Hebda and K. Pielichowski, Polyurethane/POSS hybrid materials, in *Polymer/POSS Nanocomposites and Hybrid Materials: Preparation, Properties, Applications*, ed. Kalia, S. and Pielichowski K., Springer, 2018, 167–204, DOI: 10.1007/978-3-030-02327-0_5.
24 L. V. Karabanova, V. A. Bershtein, T. E. Sukhanova, P. N. Yakushev, L. M. Egorova, E. D. Lutsyk, A. V. Svyatyna and M. E. Vylegzhanina, *J. Polym. Sci.*, 2008, **46**, 1696–1712.
25 L. V. Karabanova, R. L. D. Whitby, V. A. Bershtein, A. V. Korobeinyk, P. N. Yakushev, O. M. Bondaruk, A. W. Lloyd and S. V. Mikhalovsky, *Colloid Polym. Sci.*, 2013, **291**, 573–583.
26 L. V. Karabanova, R. L. D. Whitby, A. Korobeinyk, O. Bondaruk, J. P. Salvage, A. W. Lloyd and S. V. Mikhalovsky, *Compos. Sci. Technol.*, 2012, **72**, 865–872.
27 K. Madhavan and B. S. R. Reddy, *J. Membr. Sci.*, 2009, **342**, 291–299.
28 S. S. Mahapatra, S. K. Yadav and J. W. Cho, *React. Funct. Polym.*, 2012, **72**, 227–232.
29 J. P. Lewicki, K. Pielichowski, M. Jancia, E. Hebda, R. L. F. Albo and R. S. Maxwell, *Polym. Degrad. Stab.*, 2014, **104**, 50–56.
30 K. Wei, L. Wang and S. Zheng, *Polym. Chem.*, 2013, **4**, 1491–1501.
31 S. Bourbigot, T. Turf, S. Bellayer and S. Duquesne, *Polym. Degrad. Stab.*, 2009, **94**, 1230–1237.
32 J. Huang, P. Jiang, X. Li and Y. Huang, *J. Mater. Sci.*, 2015, **51**, 2443–2452.
33 L. V. Karabanova, L. A. Honcharova, V. I. Sapsay and D. O. Klymchuk, *Chem., Phys. Technol. Surf.*, 2016, **7**, 413–420.
34 L. V. Karabanova, L. A. Honcharova, N. V. Babkina, V. I. Sapsay and D. O. Klymchuk, *Polym. Test.*, 2018, **69**, 556–562.
35 W. Wang, Y. Guo and J. U. Otaigbe, *Polymer*, 2009, **50**, 5749–5757.
36 Y. S. Lai, C. W. Tsai, H. W. Yang, G. P. Wang and K. H. Wu, *Mater. Chem. Phys.*, 2009, **117**, 91–98.
37 E. Huitron-Rattinger, K. Ishida, A. Romo-Uribe and P. T. Mather, *Polymer*, 2013, **54**, 3350–3362.
38 L. V. Karabanova, A. W. Lloyd and S. V. Mikhalovsky, 3-D Artificial nanodiamonds containing nanocomposites based on hybrid polyurethane-poly(2-Hhydroxyethyl methacrylate) polymer matrix, in *Nanoplasmonics, Nano-Optics, Nanocomposites, and Surface Studies*, ed. Fesenko, O. and Yatsenko, L., Springer Proceedings in Physics, 2015, vol. 167, pp. 149–164, DOI: 10.1007/978-3-319-18543-9_9.
39 L. V. Karabanova, L. M. Sergeeva and G. Boiteux, *Compos. Interfaces*, 2001, **8**, 207–219.
40 L. V. Karabanova, Yu. P. Gomza, S. D. Nesin, O. M. Bondaruk, E. P. Voronin and L. V. Nosach, Nanocomposites based on multicomponent polymer matrices and nanofiller densil for biomedical application, in *Nanophysics, Nanophotonics, Surface Studies and Application*, ed. Fesenko, O. and Yatsenko, L., Springer Proceedings in Physics, 2016, vol. 183, pp. 451–475, DOI: 10.1007/978-3-319-30737-4_38.
41 L. V. Karabanova, V. A. Bershtein, Yu. P. Gomza, D. A. Kirilenko, S. D. Nesin and P. N. Yakushev, *Polym. Compos.*, 2016, **39**, 263–273.
42 A. Kausar, POSS-based IPN nanocomposites, in *Polyhedral Oligomeric Silsesquioxane (POSS) Polymer Nanocomposites: from Synthesis to Applications*, ed. Thomas, S. and Somasekharan, L., Elsevier, 2021, pp. 195–203, DOI: 10.1016/B978-0-12-821347-6.00014-7.
43 V. A. Bershtein, P. Pissis, T. E. Sukhanova, L. V. Karabanova, P. N. Yakushev, O. M. Bondaruk, P. Klonos, E. Spyratou, M. E. Vylegzhanina and E. F. Voronin, *Eur. Polym. J.*, 2017, **92**, 150–164.
44 P. Klonos, V. Chatzidogiannaki, K. Roumpos, E. Spyratou, P. Georgiopoulos, E. Kontou, P. Pissis, Yu. Gomza, S. Nesin, O. Bondaruk and L. Karabanova, *J. Appl. Polym. Sci.*, 2016, **133**, 2635–2650.
45 L. V. Karabanova, G. Boiteux, O. Gain, G. Seytre, L. M. Sergeeva and E. D. Lutsyk, *Polym. Int.*, 2004, **53**, 2051–2058.

46 S. J. Gregg and K. S. W. Sing, *Surface Area and Porosity*, Academic Press Inc., London, 2nd edn, 1982, ISBN 0-12-300956-1.
47 A. A. Tager, *Physical Chemistry of Polymers*, Mir Publishers, Moscow, 1978, ISBN-10 0714712361, ISBN-13 978-0714712369.
48 Y. S. Lipatov and L. M. Sergeeva, *Interpenetrating Polymer Networks*, Naukova dumka, Kiev, 1979.
49 D. R. Paul and S. Newman, *Polymer Blends*, Academic Press, Elsevier, Science & Technology Books, 1978, vol. 2, ISBN: 9780323149778.
50 Y. S. Lipatov and V. F. Rosovitsky, *Physical Chemistry of Multicomponent Polymer Systems*, Naukova dumka, Kiev, 1986, vol. 2.
51 L. V. Karabanova, L. A. Honcharova, N. V. Babkina and D. O. Klymchuk, *Polym. J.*, 2023, **45**, 181–194.
52 L. V. Karabanova, L. A. Honcharova and V. I. Shtompel, *Polym. J.*, 2020, **42**, 85–95.
53 X. He, M. Qu and X. Shi, *J. Mater. Sci. Chem. Eng.*, 2016, **4**, 15–22.
54 S. Chang, Z. Cunbin, X. Lihuan and Z. Cheng, *J. Macromol. Sci.*, 2015, **54**, 177–189.
55 X. Y. Shi, W. N. Bi and S. G. Zhao, *J. Appl. Polym. Sci.*, 2012, **124**, 2234–2239.